

UC Irvine

UC Irvine Previously Published Works

Title

Observations of chemical effects accompanying pulverized coal thermal decomposition

Permalink

<https://escholarship.org/uc/item/9f4598p8>

Journal

Fuel, 67(9)

ISSN

0016-2361

Authors

Kramlich, John C
Seeker, William Randall
Samuelsen, Gary S

Publication Date

1988-09-01

DOI

10.1016/0016-2361(88)90034-8

Copyright Information

This work is made available under the terms of a Creative Commons Attribution License, available at <https://creativecommons.org/licenses/by/4.0/>

Peer reviewed

Observations of chemical effects accompanying pulverized coal thermal decomposition

John C. Kramlich, William Randall Seeker and Gary S. Samuelsen*

Energy and Environmental Research Corporation, 18 Mason, Irvine, CA 92718, USA

* Department of Mechanical Engineering, University of California, Irvine, CA 92717, USA

(Received 21 September 1987; revised 23 December 1987)

A thermal decomposition reactor is used to simulate the environment of a practical coal burner and assess the influence of fuel properties on the chemical behaviour that accompanies the thermal decomposition of pulverized coal particles. The present study complements and extends previous work that explored the physical and thermal behaviour. The rate of component burnout is determined for hydrogen, nitrogen and carbon as well as the evolution of NO and HCN, and the efficiency of fuel nitrogen conversion. The results demonstrate a significant dependency on coal particle size and coal type. Modelling demonstrates that the penetration of oxygen into the fuel-rich devolatilization cloud depends on particle size and coal properties and, as a result, controls to a large extent the evolution and transformation of the chemical constituents associated with the parent fuel.

(Keywords: thermal decomposition; chemical properties; scanning electron microscopy)

The combustion of pulverized coal consists of a series of interrelated physical, thermal and chemical phenomena, each of which must be understood if the combustion is to be made efficient and the resulting pollutant formation is to be minimized. In a previous study¹, the first two of these three phenomena were examined by injecting coal particles into a hot combustion gas stream. Physical effects were studied *in situ* by laser holography, spark shadowgraphs, high-speed cinematography and scanning electron microscopy of extracted solid samples. Thermal effects were observed by two-colour pyrometry for solids temperatures, and thermocouple and sodium D-line reversal for gas temperature. This initial study showed that the significant events occur in three stages. Particles heat to the gas temperature in < 10 ms, devolatilization occurs between 10 and 75 ms, and char oxidation occurs for times exceeding 75 ms. For large bituminous particles ($\approx 80 \mu\text{m}$), a significant volatile fraction is ejected from the particle as jets, as evidenced by blowhole formation. These volatiles react in the immediate vicinity of the coal particle, producing a cloud of small, solid particles.

The local heat released during the reaction of the volatiles, in combination with heterogeneous oxidation, increases the particle surface temperature and/or the temperature in the immediate vicinity of the coal particle and raises it above that of the bulk gas stream. At longer times, large soot structures are formed, which are attributed to the agglomeration of small, homogeneously formed soot particles. Small bituminous particles ($\approx 40 \mu\text{m}$) burn with a higher intensity, at a higher temperature and more rapidly and do not produce soot structures.

Other ranks of coal exhibit different physical, thermal and chemical behaviour. For example, neither the lignites nor the anthracite produce soot structures. Further, the particle temperature for the lignites is only slightly shifted

above the bulk gas temperature in the devolatilization region while anthracite takes 50 ms to reach the bulk gas temperature level. This is attributable to the relatively low heat content of the volatiles in the former case and the low volatile content in the latter.

The object of the present study is to complement these observations with an examination of the chemical behaviour that accompanies the thermal decomposition of pulverized coal particles. The solid-phase composition change during thermal decomposition, the gas-phase composition in the vicinity of the coal particles during thermal decomposition, and the effect of particle size and coal type were studied.

The decomposition of coal has been greatly studied, while only a few studies deal with the chemical composition of the evolved gases and the char under conditions that approximate those found in pulverized coal combustion. The criteria proposed by Badzioch² for designing such an experiment include the use of realistic heating rates, reaction times and particle sizes. These criteria are normally met by entrained flow/drop tube experiments and by heated grid experiments.

In the grid experiments, a sample of the coal is contacted with an electrically heated mesh grid or gauze³⁻⁸. A heated stage (e.g. a graphite ribbon⁹) can also be used. The volatile products are expelled into cold inert gas or into a vacuum from which they are analysed. Many of these studies have been generalized to yield kinetic models of the observed behaviour^{4,6-8}. The flow reactor approach has been used in inert environments^{10,11} and under oxidizing conditions¹¹. The flow reactor approach was also used to obtain the kinetics of char weight loss during pyrolysis¹², and to follow the loss of the various char elements with time¹³.

The present study is designed to explore behaviour within an environment that is chemically and thermally

similar to that of a pulverized coal burner. As such, it couples devolatilization with volatile combustion by exposing the particles to a hot, oxidizing gas stream. The object is to provide information on char composition and on the products of the devolatilization/volatile combustion reaction.

EXPERIMENTAL

A detailed description of the reactor is provided elsewhere¹. In general terms, the reactor (*Figure 1*) consists of a sintered bronze flat-flame burner downfired into a 7.6 cm square chimney. The burner is fired on a CH₄/air mixture at atmospheric pressure, a cold gas velocity of 22.5 cm/s, and a fuel-air equivalence ratio of 0.73. The temperature downstream of the flame zone is 1750 K, and the gas experiences a linear quench of 1500 K s⁻¹ through the reaction zone. Pulverized coal is injected from a fluidized bed feeder through a hole in the centre of the flame holder and into the combustion gas. By proper manipulation of the fluidized bed controls, particle entry velocities can be varied independently of coal mass flow. The nominal coal flow rate is 0.4 g min⁻¹ with an injection velocity equal to the hot gas velocity.

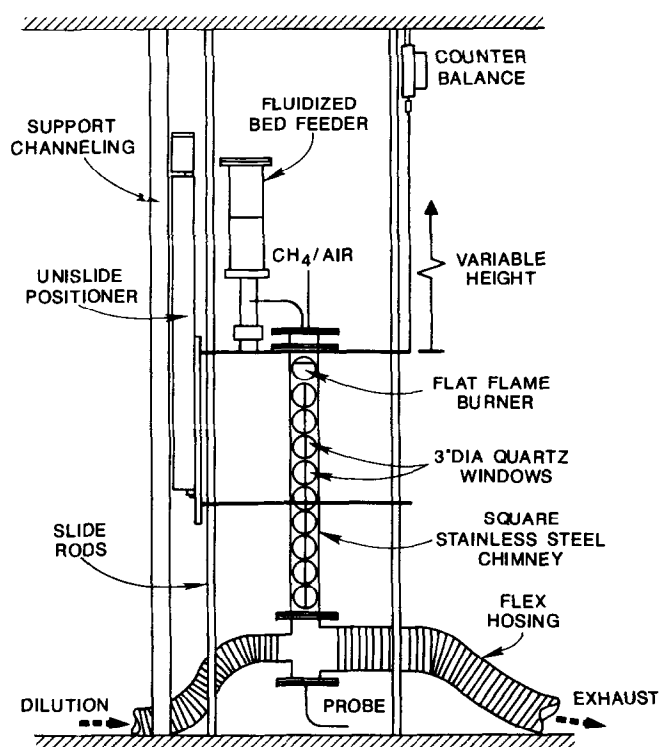


Figure 1 Reactor system¹

The solid and gas samples were obtained by a hot-water cooled stainless steel probe. Solids were removed from the sample stream by a cyclone and a fine sintered stainless steel filter. Elemental analysis of the collected solids was performed using a Perkin-Elmer 240B Elemental Analyser. Values were reported for carbon, hydrogen, nitrogen and ash. Gas samples were analysed for CO and CO₂ by NDIR analysers; oxides of nitrogen were determined by chemiluminescence. Molecular oxygen was measured using a paramagnetic analyser. Before entering each of these analysers, water vapour was condensed and removed.

Unburned hydrocarbons were determined by flame ionization gas chromatography (Perkin-Elmer Sigma 2). Gas samples were obtained in 500 cm³ evacuated flasks and subsequently injected through the g.c. sample valve for analysis. Ammonia and HCN were scrubbed from the gas stream by miniature bubblers. For these measurements, the entire sample stream, including solids, was used. Measurements of NH₄⁺ and HCN in the liquid phase were performed with specific ion electrodes. Lead carbonate was added to the bubbler solution to remove the sulphate ion interference from the HCN electrode.

RESULTS AND DISCUSSION

Results for five coals are presented: two lignites, two high volatile bituminous and an anthracite. The coal properties are summarized in *Table 1*. The Four Corners coal was aerodynamically classified into 40 and 80 μm cuts whereas the remaining coals were used as pulverized. In addition, a partially devolatilized material was prepared by passing the 80 μm Four Corners coal through the reactor and collecting all solid matter below the reaction zone.

Component burnout profiles

A typical solids composition profile is shown in *Figure 2* as a function of the axial distance from the burner, in this case for the 40 μm Four Corners coal. While these results indicate trends, the elemental analysis of the collected solids are best interpreted in terms of 'component burnout' (the mass of a given component lost by the solid compared with the mass in the parent solid), which is calculated from an elemental analysis of the collected solids.

The component burnout for hydrogen as a function of distance from injection for the various coals is shown in *Figure 3*. For the 40 μm Four Corners coal, hydrogen removal is rapid, occurring in about 30 ms, and complete, with about 95% of the original hydrogen removed. The Utah bituminous and 80 μm Four Corners coals show a two-stage behaviour with initial, rapid hydrogen burnout

Table 1 Coal analysis

Location	Rank	Proximate analysis (wt %)				Ultimate analysis (dry, wt %)		
		Volatile matter	Fixed carbon	Moisture (as received)	Ash	Carbon	Hydrogen	Nitrogen
Savage, Montana	Lignite	32.8	35.2	26.7	5.3	64.9	4.0	1.1
Beulah, North Dakota	Lignite	32.2	34.9	24.9	8.0	65.2	3.9	0.9
Four Corners, New Mexico	High volatile, b bituminous	39.3	39.0	3.8	17.9	63.4	5.3	1.5
Utah	High volatile, b bituminous	39.0	45.2	6.9	8.9	72.2	5.7	1.5
Hazleton, Pennsylvania	Anthracite	3.6	83.1	5.1	8.2	84.2	1.7	0.7

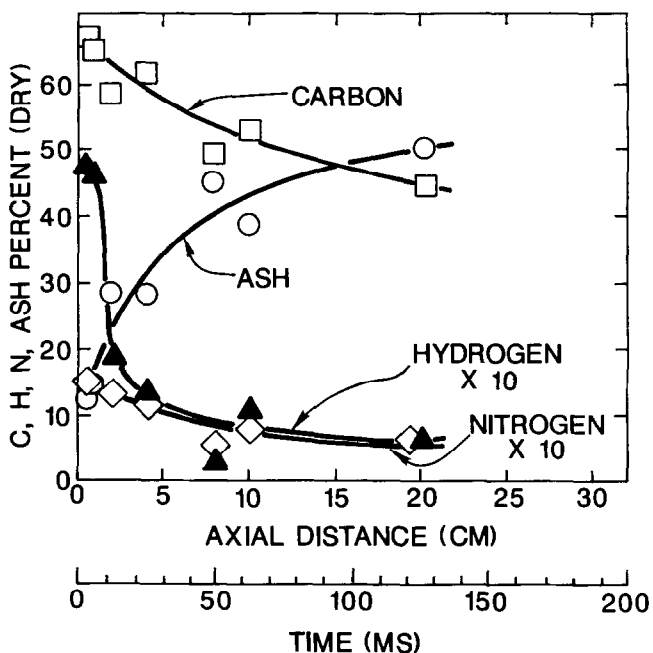


Figure 2 Solid phase composition profile of 40 μm Four Corners coal

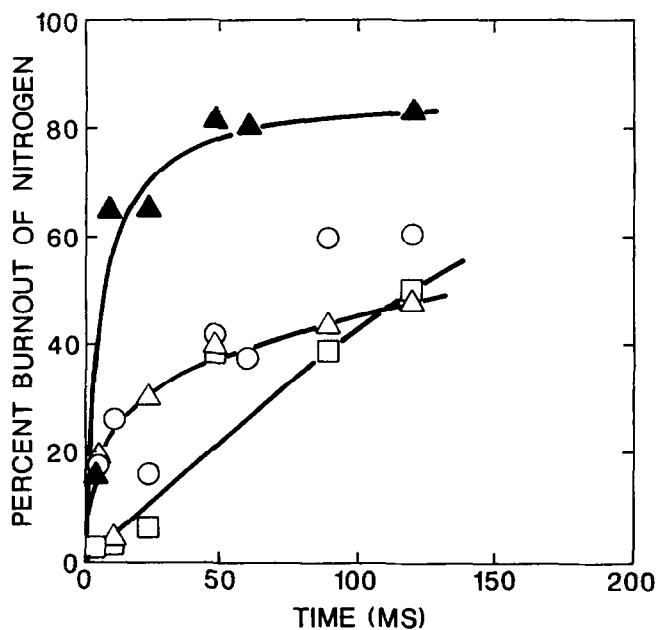


Figure 4 Burnout of nitrogen as a function of distance: Δ , 80 μm Four Corners; \blacktriangle , 40 μm Four Corners; \circ , Utah bituminous; \square , Savage lignite

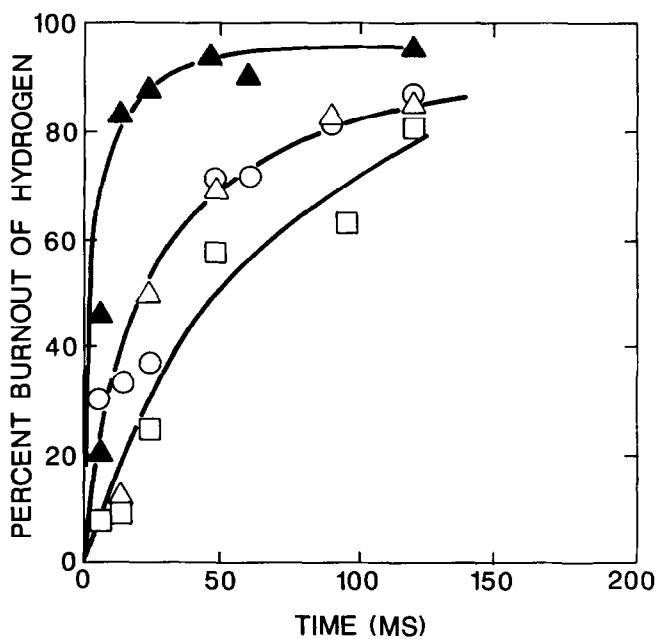


Figure 3 Burnout of hydrogen as a function of distance: Δ , 80 μm Four Corners; \blacktriangle , 40 μm Four Corners; \circ , Utah bituminous; \square , Savage lignite

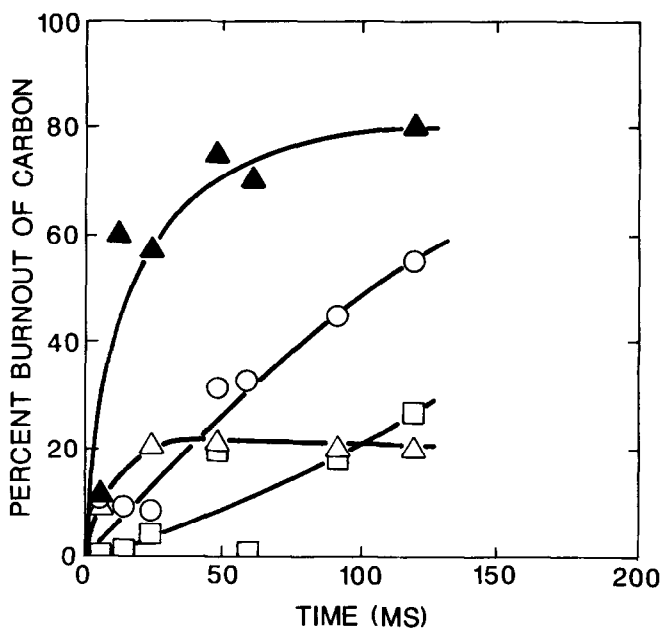


Figure 5 Burnout of carbon as a function of distance: Δ , 80 μm Four Corners; \blacktriangle , 40 μm Four Corners; \circ , Utah bituminous; \square , Savage lignite

which becomes a more gradual removal at around 50 ms. Lignites, as illustrated by the Savage profile, exhibit the more uniform burnout of hydrogen.

A similar component burnout plot for nitrogen is shown in Figure 4. Again, almost all chemical activity for the 40 μm Four Corners coal is completed within 30 ms. However, 20% of the nitrogen remains in the char. The Four Corners and Utah bituminous coals again show similar behaviour, with an early, rapid nitrogen loss corresponding to devolatilization followed by a gradual char-nitrogen removal zone. The Savage lignite loses nitrogen in an essentially linear fashion.

The burnout of carbon (Figure 5) was slightly less rapid in the devolatilization zone compared with the other components for the 40 μm Four Corners coal. In spite of slower burnout, 80% of the carbon was removed. The 80 μm Four Corners coal showed 20% carbon removal in the devolatilization zone, apparently followed by no further reaction. This is curious behaviour because Figure 3 shows that hydrogen loss continues beyond the point where carbon evolution ceases. One difference between the 80 μm Four Corners coal and the others is that it is the only bituminous coal from which the fine particles have been removed. Subsequent discussion will suggest that

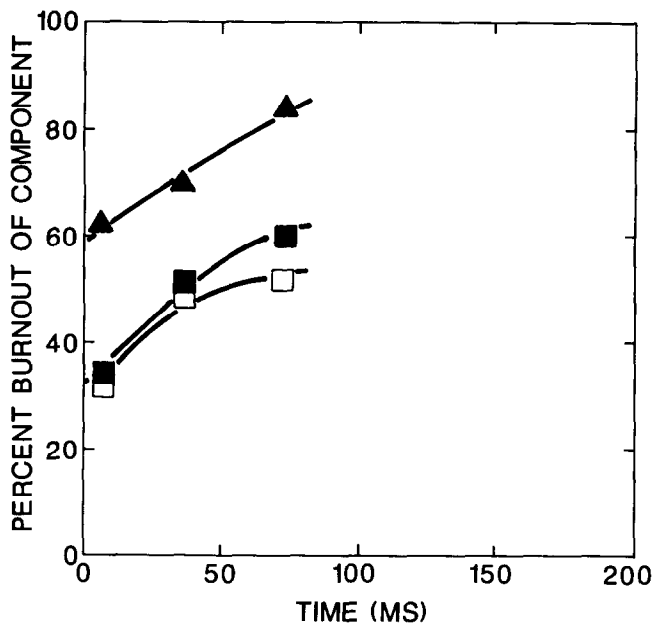


Figure 6 Burnout of 80 μm Four Corners bituminous char as a function of distance: ▲, hydrogen; ■, nitrogen; □, carbon

the gas-phase environment at the surface of the large bituminous particles is substantially different from that of the other particles. The Utah bituminous and the Savage lignite showed linear burnout profiles, with the bituminous rate twice that of the lignite. The Pennsylvania anthracite showed very little evidence of reaction throughout the burner. As a result, data for this coal are not presented.

Figure 6 shows the component burnout and elemental analysis profile for the 80 μm Four Corners bituminous char. The component burnouts are based on the parent coal, so these results represent a 'continuation' of Figures 3-5 (of course, with a repeat of the time-temperature history). The burnout of carbon increases from 20 to 50%, nitrogen from 40 to 60% and hydrogen from 60 to 80%. All burnout rates are slow relative to the behaviour of the parent coal. This is expected since the bulk of the easily volatilized material was released during the initial exposure to high temperature.

The following features arise from comparisons between the coals. Only the 40 μm Four Corners coal can be considered to be truly 'burned out'. Most of the hydrogen loss from this coal appears to be coupled to devolatilization, while the somewhat slower losses of nitrogen and carbon appear to be a combination of devolatilization and char burnout. The bituminous coals are exemplified by a well-defined devolatilization zone; lignites appear to decompose more slowly and lose volatile matter at a relatively constant rate throughout the reactor residence time. The relative burnout within a given coal was always greatest for hydrogen and least for carbon.

Gas phase composition profiles

Measurements were also made in the thermal reactor to determine the impact of coal type on NO formation, reduced nitrogen species and hydrocarbon species. The results for O₂, NO and CO₂ are presented as mole fractions for an isokinetic sample obtained at the plume centreline. For those species (hydrocarbon and HCN)

associated solely with the coal plume, the probe flow rates were set sufficiently high to ensure capture of the entire coal plume. By sampling the entire plume, the results could be presented as mass hydrocarbon or HCN per unit mass parent coal. Verification that the entire plume was collected was obtained by varying the probe flow and calculating g HCN s⁻¹ collected. Complete collection was assured when the HCN collected no longer changed with flow rate.

The gas-phase composition profiles for the 40 μm Four Corners coal are shown in Figure 7. Important features include a peak NO value of 500 ppm, a rapid decline in O₂ entering with the coal to 4%, the background reactor value and relatively low total hydrocarbon values. The HCN peak corresponds to 1.2 × 10⁻² g HCN/g parent coal. Figure 8 shows similar composition profiles for the 80 μm Four Corners coal. Maximum values for NO (480 ppm) were similar to the 40 μm coal, however, the peak location was significantly displaced downstream. Further evidence of the longer time constants involved in the 80 μm particle chemistry, relative to the 40 μm particles, include longer O₂ decay, greater time required for CO to build to a maximum and the downstream displacement of the HCN peak. Hydrocarbon levels are also considerably elevated. The 80 μm char produced an NO profile similar in shape to the parent coal, although the maximum was only 300 ppm compared with the previous 480 ppm (Figure 9). Although CO, HCN and hydrocarbons were measured for this material, the results showed insignificant concentrations, and these were not plotted. Also, the O₂ concentration did not vary from its background value.

The gas phase profiles for the Utah bituminous coal (Figure 10) are strikingly similar to those for the 80 μm Four Corners coal. Although absolute values are different, the profile shapes are generally similar.

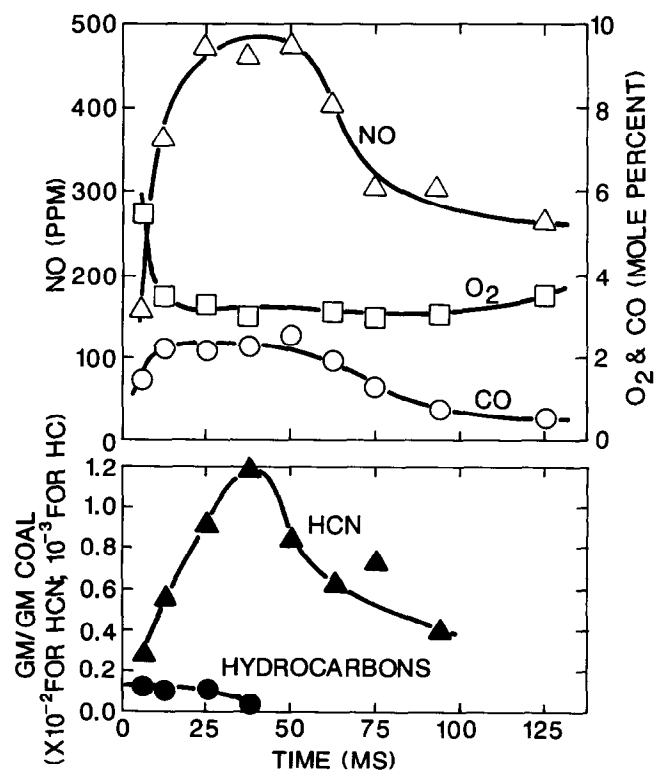


Figure 7 Gas phase composition profiles for 40 μm Four Corners bituminous

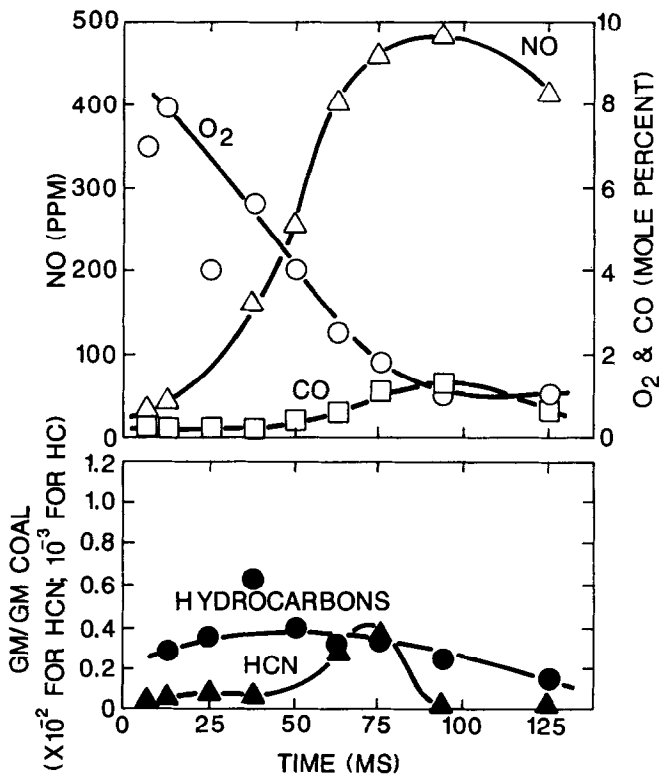


Figure 8 Gas phase composition profiles for 80 μm Four Corners bituminous

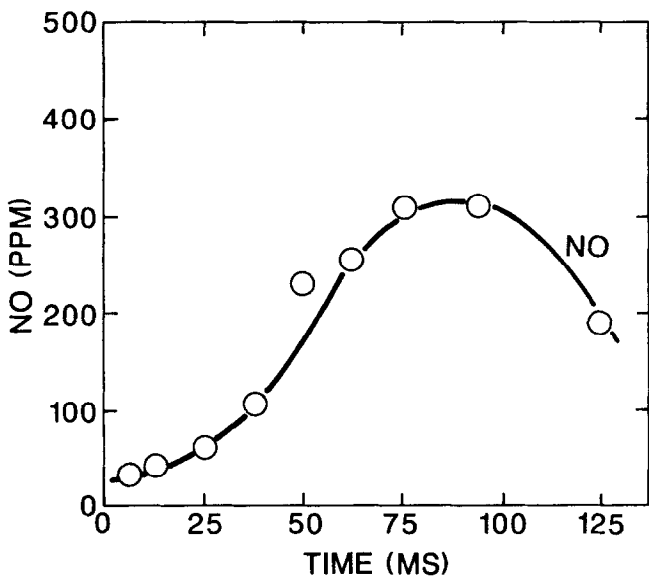


Figure 9 Gas phase composition profile for 80 μm Four Corners bituminous char

However, NO peaks earlier. This is attributed to the fine coal particles that are present in the Utah coal but have been removed from the 80 μm Four Corners coal. The lower absolute value of NO is attributed to the higher predominance of reducing hydrocarbon in the volatile cloud.

The lignites show surprisingly similar NO behaviour to the bituminous coals, as illustrated in Figure 11 for the Savage lignite. However, CO and HCN were considerably depressed. In addition, hydrocarbons were totally absent, which may explain the high conversion of fuel nitrogen to NO. The anthracite yielded minimal NO_x

(80 ppm), very low CO and no measurable volatile species (hydrocarbons, HCN, NH₃).

Conversion efficiency of fuel nitrogen

The conversion efficiency of fuel nitrogen can be further explored by measurements of NO in the stack, well after the chemistry and mixing have fixed the flue gas

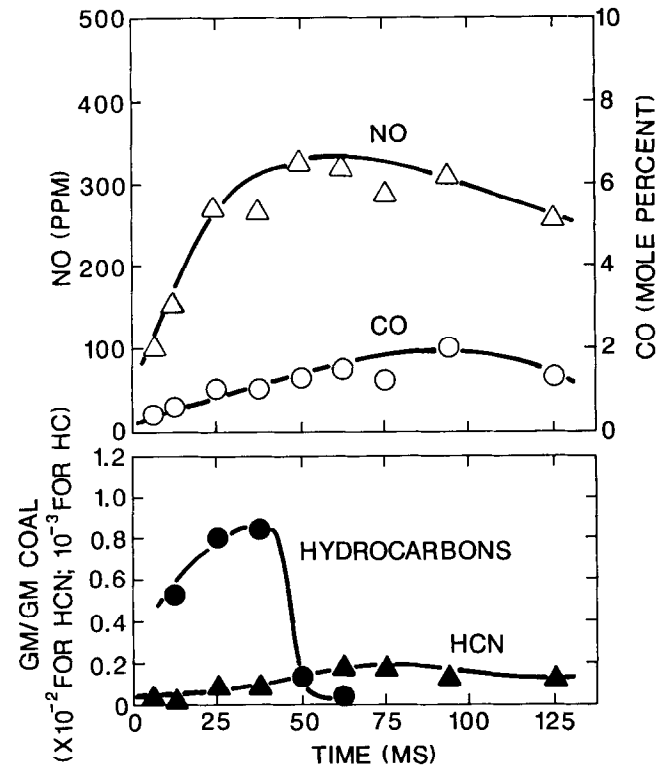


Figure 10 Gas phase composition profiles for Utah bituminous

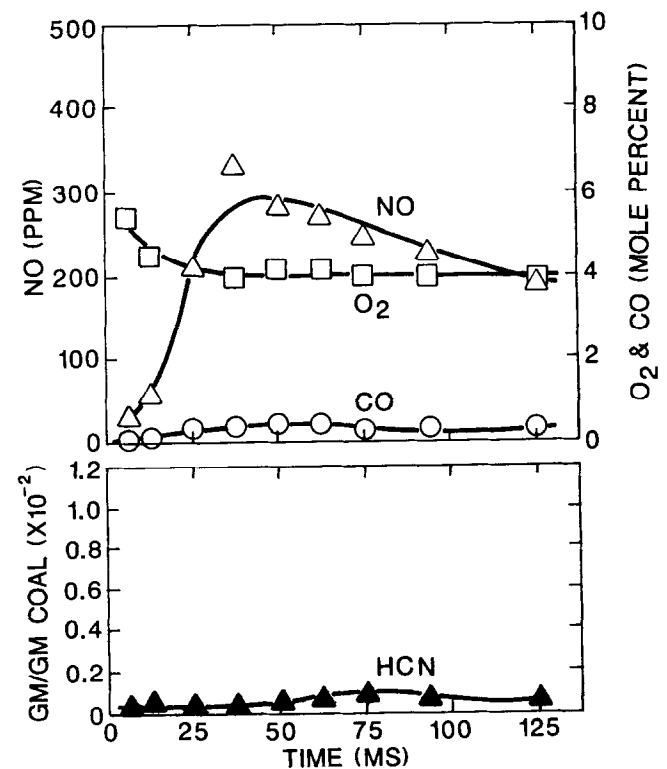


Figure 11 Gas phase composition profiles for Savage lignite

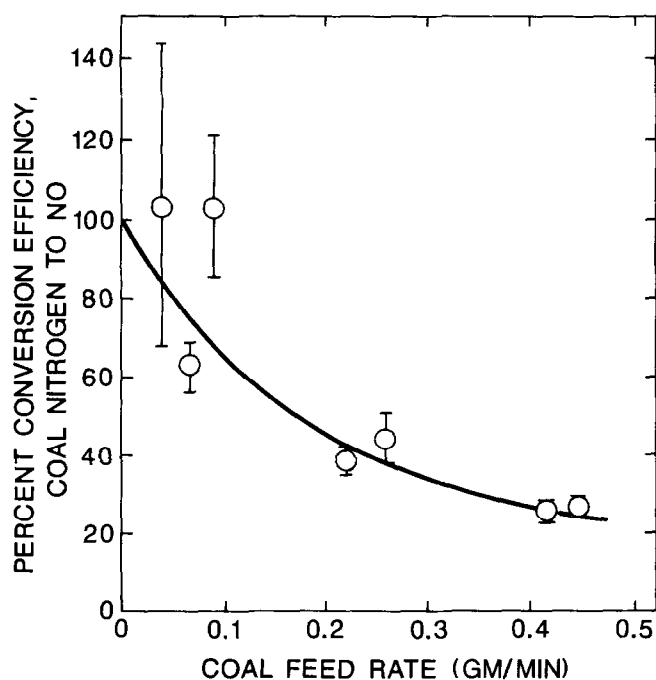


Figure 12 Conversion efficiency of coal-nitrogen to NO for 40 μm Four Corners bituminous

concentration. For example, stack NO measurements (Figure 12) for the 40 μm New Mexico bituminous coal demonstrate a very strong dependence of NO produced on the coal feed rate. Conversion efficiencies of fuel nitrogen to NO, determined from the particulate matter composition profiles and the stack NO measurements, vary from $\approx 100\%$ at low flow rates to almost 20% at medium flow rates. These data imply that, at low feed rates when particles are bathed in the oxygen-rich background gas and separated from the influence of other coal particles, the conversion efficiency is very high. This suggests almost complete oxidation of the nitrogen volatiles to NO under oxidizing conditions in the volatile cloud/particle microsystem. Lower conversion efficiencies are likely to occur at higher coal flow rates because the devolatilization products from many particles combine to produce a surrounding gaseous environment with high concentrations of nitrogen species and low or zero oxygen concentrations. For the larger ($\approx 80 \mu\text{m}$) bituminous particles the conversion efficiency at low feed rates approaches only 65%.

Kinetic modelling

The previous data suggests that the chemistry in the immediate vicinity of the coal particle can strongly influence the efficiency of conversion of released nitrogen to NO. To gain some insight into these processes, a chemical kinetic model was applied to the diffusion flame surrounding the coal particle. The model included the following elements:

1. A solution of the finite difference forms of the energy, momentum and species conservation equations in the spherically symmetric domain bounded by the particle surface, and an arbitrarily large radius^{1,4}.
2. The chemistry governed by detailed chemical kinetics^{1,5}, including nitrogen and hydrocarbon reactions.

3. The species flux into the domain (i.e. matter leaving the coal particle) is set at the rate measured in this study, and the composition of these volatiles are selected from heated grid experiments^{4,6}.
4. The solution is time-varying, with the initial particle temperature as 300 K, and the domain set at the free stream temperature of 1750 K. The initial and free stream composition is set at the equilibrium value, except for NO, which is set to zero to avoid contaminating the calculation with an unrealistically high equilibrium concentration.

Figure 13 shows the radial profiles for temperature, oxygen and methane. The results show a rapid approach to a steady state spherical combustion cloud about the coal particle; less than 1 ms of the total devolatilization time was required. It is important to note that there was no provision for endothermic devolatilization reactions. The coal particle was allowed to float at the adjoining gas stream temperature. However, this does not represent a major limitation because the devolatilization rates were externally imposed and, therefore, do not explicitly depend on local temperature.

Three coal types are shown in Figure 13: a 40 and 80 μm bituminous and an 80 μm lignite. The temperature overshoots for gas surrounding the bituminous coals (80 μm , 380 K; 40 μm , 355 K) and the lignite (225 K) agree favourably with the results presented previously for the two-colour measurement of the burning coals¹. The O₂ traces show the bituminous coals, and particularly the larger particles, were significantly shielded from free stream O₂. This occurs because the bituminous volatiles are of a higher quality fuel content than the lignite. Thus, the volatile reaction occurs with greater intensity in the immediate vicinity of the particle, and shields the particle by removing most of the locally available oxygen. The deeper O₂ penetration observed for the 40 μm particle is due to the smaller total mass flow of volatile gases. The lignite shows deeper O₂ penetration because the fuel content of the volatiles is concentrated in slow burning CO rather than fast burning hydrocarbons; the rate of O₂ removal is insufficient to shield the particle.

Figure 5 showed that carbon release from the 80 μm Four Corners coal ceased at 20%, while Figure 3 showed that hydrogen release continues. All the other coals studied generally show a simultaneous release of carbon and hydrogen. The 80 μm Four Corners coal is unique in that it is the only bituminous coal from which the fines have been removed. Thus, this is the only coal in which oxygen was largely excluded from the particle surface. This may imply that under the conditions studied here, the presence of some oxygen is necessary to aid in carbon release.

The CH₄ profiles indicate a zone of $\approx 1 \text{ mm}$ diameter surrounding the 80 μm bituminous particles where O₂ is depleted and CH₄ is present in excess of 1%. This region would have a large potential for soot formation, and indeed, the soot clouds previously observed for these particles are of this size¹. Note that the 40 μm bituminous and 80 μm lignite exhibit considerably lower hydrocarbon levels about the particle. This is consistent with our earlier observations of no soot cloud accompanying these particles¹.

The predictions for the principal fixed nitrogen species are shown in Figure 14 for the 80 μm bituminous coal. The HCN and NH₃ that are evolved from the particle are

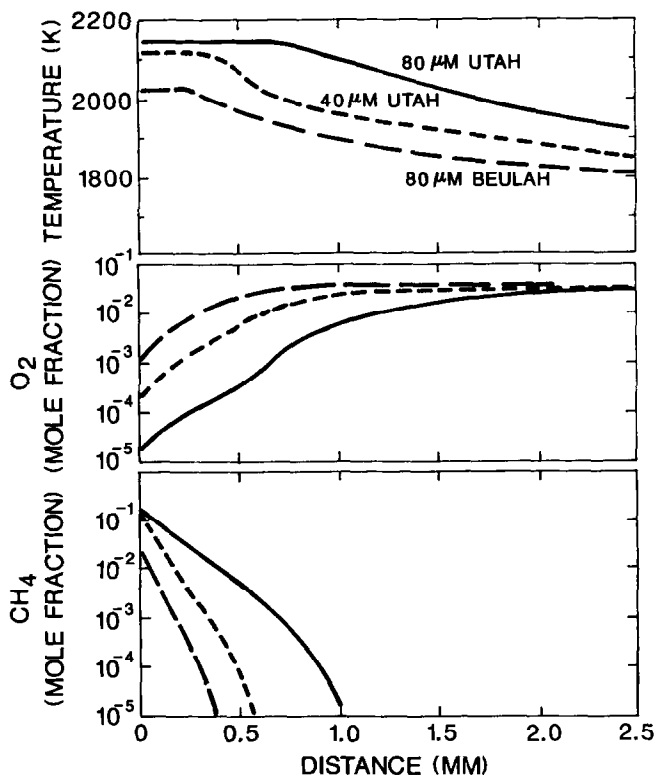


Figure 13 Results of kinetic modelling

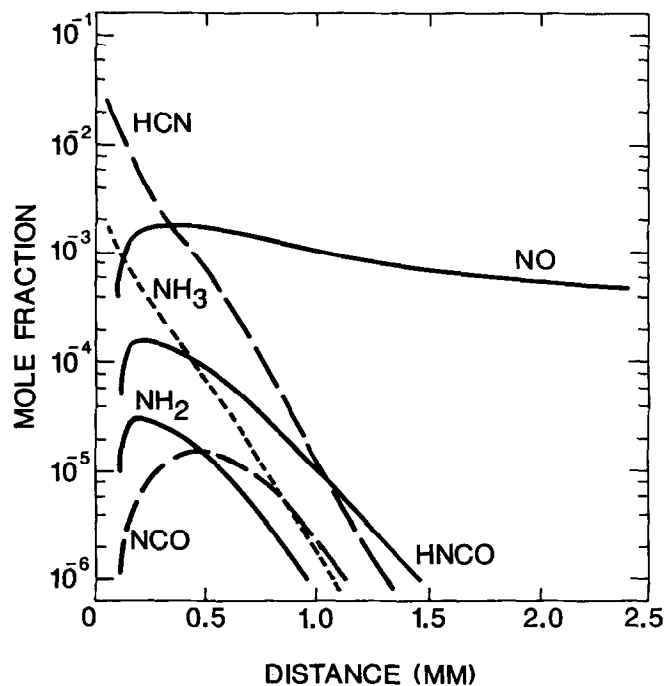


Figure 14 Fixed nitrogen profiles about an 80 μm bituminous coal particle

largely consumed within 0.5 mm of the particle surface. The decrease in NO at larger radii is due to its steady-state diffusion into an infinite medium and does not represent any chemical activity. Most of the nitrogen chemistry occurs within the region of relatively high hydrogen concentrations. In spite of the active chemistry, only an insignificant amount of fixed nitrogen is reduced

to N₂ within the volatile flame. Since only 65% of the released nitrogen was observed as NO in the single particle limit, the model suggests the existence of other mechanisms for fixed-nitrogen reduction for these large bituminous particles. One possibility is that nitrogen is reduced by heterogeneous reaction with the soot cloud that surrounds these large particles. Since the cloud was absent from the 40 μm particles, nitrogen conversion to NO would be complete, as was observed. Another possibility is that the reduced O₂ partial pressure at the particle surface leads to a highly reducing environment within the coal char. This could lead to a nitrogen reduction that may not occur for the smaller particles because of better O₂ availability throughout the char.

CONCLUSIONS

1. The rate of component burnout depends on the volatile content and composition. Bituminous coals exhibit a very rapid initial burnout of hydrogen, nitrogen and carbon associated with devolatilization whereas the lignites decompose more slowly.
2. Small New Mexico bituminous particles ($\approx 40 \mu\text{m}$) exhibited an even more rapid burnout than the larger cut ($\approx 80 \mu\text{m}$), broadly distributed, pulverized Utah coal sample.
3. Size effects are also noted in the evolution of fuel NO, with the peak concentration occurring earlier with the smaller ($\approx 40 \mu\text{m}$) particle.
4. Fuel nitrogen conversion efficiency is reduced in the presence of a high hydrocarbon content in the volatiles, larger particles that produce a cloud to restrict penetration of oxygen to the nitrogen species or low number density of particles in a surrounding oxygen-rich background gas.
5. Modelling of the cloud/particle microsystem successfully explained the results by demonstrating first, that the penetration of the oxygen-rich background gas can determine the extent to which soot and NO is formed within the cloud and, second, the penetration of oxygen is dictated by the size of the particle, the amount of volatile mass evolved and the composition of the volatile mass.

ACKNOWLEDGEMENTS

The authors thank the US Environmental Protection Agency for their support, through the Combustion Research Branch, Air and Energy Engineering Research Laboratory, Research Triangle Park, NC, USA.

REFERENCES

- 1 Seeker, W. R., Samuelsen, G. S., Heap, M. P. and Trolinger, J. D. 18th Symp. (Int.) on Combustion, The Combustion Institute, 1981, p. 1213
- 2 Badzioch, S. in 'Combustion of Pulverized Coal' (Eds. M. A. Field, D. W. Gill, B. B. Morgan and P. G. W. Hawksley) The British Coal Utilization Association, Leatherhead, 1967, pp. 160-1
- 3 Losin, R. and Chauvin, R. *Chem. Ind. (Paris)* 1964, 91, 269
- 4 Suuberg, E. M., Peters, W. A. and Howard, J. B. 17th Symp. (Int.) on Combustion, The Combustion Institute, Pittsburgh, 1979, 117

- 5 Suuberg, E. M., Peters, W. A. and Howard, J. B. *Ind. Eng. Chem. Proc. Des. Dev.* 1978, **17**, 37
- 6 Solomon, P. R. and Colket, M. B. 17th Symp. (Int.) on Combustion, The Combustion Institute, Pittsburgh, 1979, 131
- 7 Arendt, P. and van Heek, K. H. *Fuel* 1981, **60**, 779
- 8 Solomon, P. R. and Colket, M. B. *Fuel* 1978, **57**, 749
- 9 Blair, D. W., Wendt, J. O. L. and Bartok, W. 16th Symp. (Int.) on Combustion, The Combustion Institute, Pittsburgh, 1977, 475
- 10 Solomon, P. R., Hamblen, D. G., Carangelo, R. M. and Krause, J. L. 19th Symp. (Int.) on Combustion, The Combustion Institute, Pittsburgh, 1982, 1139
- 11 Pohl, J. H. and Sarofim, A. F. 16th Symp. (Int.) on Combustion, The Combustion Institute, Pittsburgh, 1977, 411
- 12 Scaroni, A. W., Walker, P. L. and Essenhigh, R. H. *Fuel* 1981, **60**, 71
- 13 Kobayashi, H. *PhD Dissertation*, Department of Chemical Engineering, Massachusetts Institute of Technology, Cambridge, 1976
- 14 Kau, C. J. and Tyson, T. J. in 'Fundamental Combustion Research Applied to Pollution Formation: Vol. 4, Engineering Analysis', EPA-600/7-87-027, US Environmental Protection Agency, 1987
- 15 Seeker, W. R., Heap, M. P., Tyson, T. J., Kramlich, J. C. and Corley, T. L. in 'Fundamental Combustion Research Applied to Pollution Formation: Vol. 1, Gas-Phase Chemistry', EPA-600/7-85-048, US Environmental Protection Agency, 1985